Published in final edited form as:

Nature. 2016 October 06; 538(7623): 79–83. doi:10.1038/nature19089.

Surface patterning of nanoparticles with polymer patches

Rachelle M. Choueiri[1], **Elizabeth Galati**[1], **Héloïse Thérien-Aubin**[1], **Anna Klinkova**[1], **Egor M. Larin**[1], **Ana Querejeta-Fernández**[1], **Lili Han**[2,3], **Huolin L. Xin**[2], **Oleg Gang**[2], **Ekaterina B. Zhulina**[4,5], **Michael Rubinstein**[6], and **Eugenia Kumacheva**[1,7,8]

[1]Department of Chemistry, University of Toronto, 80 Saint George Street, Toronto, Ontario M5S 3H6, Canada

[2]Center for Functional Nanomaterials, Brookhaven National Laboratory, Upton, New York 11973, USA

[3]Institute of New Energy Materials, School of Materials Science and Engineering, Tianjin University, Tianjin 300072, China

[4]Institute of Macromolecular Compounds of the Russian Academy of Sciences, Saint Petersburg, 199004, Russia

[5]Saint Petersburg National University of Informational Technologies, Mechanics and Optics, Saint Petersburg, 197101, Russia

[6]Department of Chemistry, University of North Carolina, Chapel Hill, North Carolina 27599-3290, USA

[7]Institute of Biomaterials and Biomedical Engineering, University of Toronto, 4 Taddle Creek Road, Toronto, Ontario M5S 3G9, Canada

[8]Department of Chemical Engineering and Applied Chemistry, University of Toronto, 200 College Street, Toronto, Ontario M5S 3E5, Canada

Abstract

Patterning of colloidal particles with chemically or topographically distinct surface domains (patches) has attracted intense research interest[1–3]. Surface-patterned particles act as colloidal analogues of atoms and molecules[4,5], serve as model systems in studies of phase transitions in

Correspondence and requests for materials should be addressed to E.K. (ekumache@chem.utoronto.ca).

Supplementary Information is available in the online version of the paper.

Author Contributions E.K. and R.M.C. proposed the approach and designed the experiments for nanoparticle surface patterning. R.M.C. synthesized and surface-patterned polystyrene-coated gold nanospheres, nanodumbbells and nanorods, and conducted self-assembly experiments of patchy nanospheres in the presence of excess polymer. E.G. synthesized and surface-patterned polystyrene-capped gold nanospheres and silver nanocubes, as well as poly (*N*-vinyl carbazole)-functionalized nanospheres. E.G. and E.M.L. determined polystyrene grafting density on nanosphere surfaces. H.T.-A. synthesized polystyrene-*co*-PI and poly(4-vinyl pyridine) and surface-patterned nanosphere surfaces. R.M.C., E.G. and H.T.-A. statistically characterized the morphology of patchy nanospheres. A.K. synthesized triangular silver nanoprisms and nanocubes and conducted experiments on nanocube self-assembly. A.Q.-F. surface-patterned gold nanocubes and conducted self-assembly of patchy nanospheres. L.H. performed tomography experiments and H.L.X. and O.G. interpreted the data. E.B.Z. and M.R. developed the theoretical model describing polymer segregation on the nanosphere surface.

The authors declare no competing financial interests.

liquid systems[6], behave as 'colloidal surfactants'[7] and function as templates for the synthesis of hybrid particles[8]. The generation of micrometre- and submicrometre-sized patchy colloids is now efficient[9–11], but surface patterning of inorganic colloidal nanoparticles with dimensions of the order of tens of nanometres is uncommon. Such nanoparticles exhibit size- and shape-dependent optical, electronic and magnetic properties, and their assemblies show new collective properties[12]. At present, nanoparticle patterning is limited to the generation of two-patch nanoparticles[13–15], and nanoparticles with surface ripples[16] or a 'raspberry' surface morphology[17]. Here we demonstrate nanoparticle surface patterning, which utilizes thermodynamically driven segregation of polymer ligands from a uniform polymer brush into surface-pinned micelles following a change in solvent quality. Patch formation is reversible but can be permanently preserved using a photocrosslinking step. The methodology offers the ability to control the dimensions of patches, their spatial distribution and the number of patches per nanoparticle, in agreement with a theoretical model. The versatility of the strategy is demonstrated by patterning nanoparticles with different dimensions, shapes and compositions, tethered with various types of polymers and subjected to different external stimuli. These patchy nanocolloids have potential applications in fundamental research, the self-assembly of nanomaterials, diagnostics, sensing and colloidal stabilization.

We hypothesized that the segregation of polymer ligands into surface-pinned micelles having a footprint area comparable with the surface area of the nanoparticle could be used as a thermodynamically mediated strategy for the patterning of the high-curvature surface of nanocolloids. The formation of pinned micelles on planar surfaces has been studied for polymer molecules strongly grafted to a macroscopic planar surface[18–21]. When a polymer-tethered substrate was transferred from a good to a poor solvent, a smooth layer segregated into micelles composed of a dense core and stretched surface-tethered 'legs' (Fig. 1a, top).

The proposed approach to patchy nanoparticles is illustrated in Fig. 1a (bottom). On the nanoparticle surface, following the reduction in solvent quality, a uniformly thick polymer brush layer breaks up into a discrete number of pinned micelles (patches). The process is driven by attractive polymer–polymer interactions and the competition between the polymer grafting constraints and the reduction in its interfacial free energy.

Here we validate this approach for nanoparticles with different dimensions, shapes and chemical compositions, which were capped with various types of polymer and copolymer ligands and subjected to different external stimuli. We show experimentally and theoretically that the size of patches is governed by the polymer dimensions and grafting density, whereas the number of patches per nanoparticle is determined by the ratio between the nanoparticle diameter and polymer size. The patches could be permanently vitrified by polymer photocrosslinking. The resulting patchy nanoparticles acted as *in situ* colloidal surfactants and their self-assembly exhibited new binding modalities.

We note that in addition to the generation of patchy nanoparticles, polymer segregation on the surface of nanoparticles has other far-reaching implications. Polymer-tethered nanoparticles have a broad range of applications in imaging and medical diagnostics[22], therapeutics[23], and chemical sensing[24]. The change in morphology of the polymer layer

under varying ambient conditions is of fundamental importance and can be used for the efficient design of nanoparticles aimed at specific applications.

To explore the proposed approach, we synthesized gold spherical nanoparticles (nanospheres) with a mean diameter D in the range from 20 ± 1.0 nm to 80 ± 1.5 nm, which were stabilized with cetyltrimethylammonium bromide or cetylpyridinium chloride. These low-molecular-mass ligands were replaced with thiol-terminated polystyrene molecules with a molecular mass of 29,000 g mol^{-1} or 50,000 g mol^{-1} (Supplementary Figs 1–4 and Supplementary Tables 1–3). (Henceforth we refer to these polymers as polystyrene-30K and polystyrene-50K, respectively.) The polymer-capped nanospheres were dispersed in dimethylformamide (DMF), a good solvent for polystyrene molecules (the value of the second virial coefficient, A_2, is 3.5×10^{-4} mol cm^3 g^{-2}, equivalent to a Flory–Huggins interaction parameter of 0.46)[25].

Figure 1b shows a transmission electron microscopy (TEM) image of 20-nm-diameter nanospheres functionalized with polystyrene-50K. When cast on the grid from the solution in DMF, the nanospheres were engulfed by a uniformly thick polymer shell. Following the reduction in solvent quality for the polystyrene ligands—by adding water to the nanosphere solution in DMF—the polymer layer transformed into a surface patch (Fig. 1c). Since the surface mobility of thiol-terminated molecules is suppressed for multi-facet gold nanospheres and for high-molecular-mass ligands, and since their lateral motion is generally slow[26], we expected that in a poor solvent, stretched polystyrene-50K molecules would be grafted to the nanosphere surface, as is shown in Fig. 1a, bottom. Upon polymer surface segregation, the yield of patchy nanospheres was 65%; other species included small self-assembled nanosphere clusters (32%) and nanospheres with a smooth shell (3%). After removal of the clusters by centrifugation, the fraction of patchy nanospheres was about 98%. Patch formation was reversible: upon dilution of the solution with DMF to a water concentration of $C_w < 1$ vol% the core–shell nanosphere morphology was recovered.

The formation of multi-patch nanospheres was explored for nanospheres with larger dimensions. Figure 1d shows a three-dimensional electron tomography reconstruction image of the 60-nm-diameter patchy gold nanosphere capped with polystyrene-50K (see Supplementary Information for details). The nanosphere carried three polymer patches, each shown with a different arbitrary colour for clarity. The side view, obtained from tomographic reconstruction, revealed an elongated patch shape, which could be induced by the partial wetting of the substrate with the polymer solution. Some accumulation of the polymer at the nanosphere–substrate interface (Supplementary Fig. 21, Supplementary Videos 1 and 2), supports this assumption.

To ensure that polymer surface segregation occurs in solution, patchy gold nanospheres tethered with thiol-terminated random copolymer polystyrene-*co*-polyisoprene were introduced into a 0.05 wt% solution of photoinitiator azobisisobutyronitrile in the DMF/water mixture and exposed to ultraviolet irradiation for 5 min. Partitioning of the photoinitiator into the patches and copolymer photocrosslinking yielded a permanent patchy structure on the nanosphere surface, which was preserved in tetrahydrofuran, a good solvent for the copolymer (Fig. 1e). Without crosslinking, the patches transformed into a smooth

shell (Supplementary Fig. 20). Below, we refer to the non-crosslinked patchy nanoparticles, which were characterized by analysing their two-dimensional projections in TEM images.

Patch formation and their structure were governed by polymer length, nanosphere diameter, and polymer grafting density. In the first series of experiments, we examined transitions between the nanospheres with a smooth polymer shell (core–shell nanospheres) and patchy nanospheres at varying ratios between the nanosphere and polymer size. Nanospheres with diameter 20 nm ≤ D ≤ 80 nm were capped with polystyrene-30K or polystyrene-50K, having molecular radii, R, of 11 nm or 15 nm, respectively[27]. (The unperturbed polymer chain size is typically defined as the root-mean-square end-to-end distance R of a polymer in its ideal conformation, which we call here the 'chain radius' or 'molecular radius' R.) At a constant grafting density σ of polymer chains with a radius R, polymer segregation was favoured for small nanospheres (Fig. 2a, top, and Supplementary Figs 9–13 and 22–24), while the reduction in R led to a larger number of patches per nanosphere at constant D and σ (Fig. 2a, bottom). Figure 2b illustrates these trends for varying D/R ratios (characterizing a different extent of stretching of the micellar 'legs'). For example, at D/R = 1.3 (D = 20 nm, polystyrene-50K), 98% of the nanospheres had a single patch, while at D/R = 2.6 (D = 34 nm, polystyrene-50K), 34% and 53% of the nanospheres had one and two patches, respectively. The angles between the patch centres were 170° ± 9° and 120° ± 13° for two-patch and three-patch nanospheres, correspondingly, characterizing the uniformity of patch distribution on the nanosphere surface. The average maximum patch height increased with polymer molecular mass: for two-patch 40-nm-diameter nanospheres capped with polystyrene-30K and polystyrene-50K the patch height was 6.5 ± 0.65 nm and 9.0 ± 0.31 nm, respectively.

Next, the formation of patches was examined while varying the grafting density, σ, of polystyrene-50K capping nanospheres with different dimensions. Figure 2c shows the experimental diagram of nanosphere states, plotted in D–σ parameter space. The transition between the core–shell and patchy nanospheres was favoured at decreasing σ and D (or increasing curvature) values, signified by the negative slope of the boundary solid blue line. In the patchy region, the average number of patches per nanosphere, n, increased with the nanosphere diameter and did not noticeably vary with σ (and was thus averaged over the range of σ studied). The latter effect further supports the lack of lateral mobility of thiol-terminated polymer ligands on the nanosphere surface. The polymer grafting density influenced patch dimensions. For example, for three-patch nanospheres with D = 60 nm the average maximum height of the polystyrene-50K patch decreased from 7.7 ± 1.1 nm to 3.1 ± 0.35 nm when σ reduced from 0.02 to 0.003 chains per square nanometre, respectively.

The trends shown in Fig. 2c were captured in the theoretical state diagram in Fig. 2d (the theoretical model is described in Supplementary Information). The structure of the polymer layer on the nanosphere surface was governed by the polymer–solvent interfacial energy and the energy of stretching of end-tethered polymer molecules. In Fig. 2d, at high σ values (the right region of the diagram), extended polymer chains minimized their interfacial and stretching energies by forming a smooth layer[19]. At lower values of σ (the left side of the diagram), the layer became thinner than the unperturbed molecular size of the polymer and the interfacial polymer–solvent energy was lowered by polymer segregation in pinned

micelles. The elastic energy of stretched micellar ‘legs’ was comparable to the polymer–solvent interfacial energy. For large nanospheres, the transition between the two regions is shown as a blue line approaching the grafting density $\tau/(bR)$, where τ accounts for the solvent quality and b is the monomer length.

The competition between the interfacial and stretching energies resulted in the optimized micelle footprint area $A \approx (N^2\tau/\sigma)^{2/5}$, where N is the polymer degree of polymerization. Since the number of micelles per nanosphere is proportional to the ratio between the nanosphere surface area πD^2, and the micelle footprint area A, for varying nanosphere dimensions and/or polymer grafting densities, transitions were expected between the nanospheres with n and $n + 1$ patches. The inclined red lines with constant $\pi D^2/A$ ratios in Fig. 2d outline these transitions, with single-patch ($n = 1$) nanospheres at the bottom and a transition between $n = 1$ and $n > 1$ at $D \approx R$.

The effect of nanosphere size (or surface curvature) on patch formation was revealed by the position and incline of the boundary between the core–shell and patchy nanosphere states. The balance between the interfacial energy of the polymer and the free energy of stretching of the micellar ‘legs’ led to a higher stability of micelles on small nanospheres and hence a negative slope of the boundary line. Thus overall, the experimental and theoretical results were in excellent agreement.

The versatility of the nanopatterning method was explored for nanoparticles with different shapes and compositions, capped with different polymer ligands strongly binding to the nanoparticle surface and subjected to different solvents (Supplementary Figs 5–8 and 14–19). Following the prediction of the theoretical model on a stronger tendency for patch formation on surfaces with a high curvature, we examined polymer segregation on nanorods, nanocubes and triangular nanoprisms. Following incubation of polystyrene-50K-capped spherocylindrical gold nanorods in the DMF/water mixture, a uniform polymer layer separated into two distinct patches engulfing the nanorod tips (Fig. 3a). Similar polymer segregation towards metal tips occurred for gold nanorods with a dumbbell shape (Fig. 3b). Patches of polystyrene-50K formed on the edges of silver nanocubes and triangular nanoprisms incubated in a poor solvent (Fig. 3c, d), as well as on edges of gold nanocubes in the tetrahydrofuran/water mixture (Supplementary Fig. 18).

Other polymer ligands exhibited qualitatively similar surface segregation in a poor solvent. Thiol-terminated poly(4-vinyl pyridine) on gold nanospheres formed into a patch following an increase in pH of an aqueous nanosphere solution from 2.5 to 11.5, at which the polymer became hydrophobic (Fig. 3e). Thiol-terminated poly(*N*-vinyl carbazole) ligands split into two patches on the surface of gold nanospheres incubated in the DMF/water mixture (Fig. 3f).

The generation of patchy nanoparticles enabled preliminary exploration of their new self-assembly modalities. In the present work, to produce individual patchy nanoparticles, we suppressed their self-assembly in a poor solvent by using dilute solutions; however, given sufficient time, patchy nanospheres assembled in chains co-existing with small clusters of two to three single-patch nanospheres (Supplementary Fig. 25). We isolated nanosphere

dimers (shown in Fig. 4a) by centrifugation of the colloidal solution and separation of larger nanosphere assemblies. The ability to control the separation between the gold surfaces by varying polymer grafting density or molecular mass enables control over hot spots of a strong electric field in the gap between the nanospheres in the dimers, making them useful in Raman scattering[28]. Inspection of isolated chains of patchy nanospheres revealed that they were built from dimers and trimers (Fig. 4b and Supplementary Figs 25 and 26), suggesting a sequential mechanism of the self-assembly of patchy nanospheres: a faster assembly of dimers and trimers and a slower assembly of these building blocks in chains, in comparison with the self-assembly of non-patchy nanospheres[29].

A new binding modality was also observed for patchy nanocubes undergoing self-assembly in an open, ‘checkerboard’ structure, owing to the binding of nanocube edges in a poor solvent (Fig. 4c), markedly different from the face-to-face assembly of the nanocubes uniformly coated with polystyrene ligands (Supplementary Fig. 27). For patchy nanocubes, the face-to-face and the ‘checkerboard’ assembly via the formation of four bonds between the edges may result in a similar reduction in the surface free energy of the system, whereas for nonpatchy nanocubes, the formation of close-packed structures would be favoured, owing to the maximum screening of unfavourable polymer interactions with a poor solvent[30].

The amphiphilic nature of patchy nanospheres led to their assembly at the interface between immiscible liquids, thus reducing the surface energy of the system and behaving as colloidal surfactants. Following the addition of water to the mixture of polystyrene-capped gold nanospheres and non-thiolated free polystyrene molecules in DMF, the reduction in solvent quality led to the formation of patchy nanospheres and polystyrene-rich droplets. The nanospheres self-assembled on the droplet surface, with a polystyrene patch immersed in the droplet (Fig. 4c). A considerably higher energy of attachment of patchy nanospheres to liquid–liquid interface[6], in comparison with conventional Pickering emulsions, is expected to provide enhanced stabilization properties of emulsions. Sonication of patchy nanospheres and non-thiolated polystyrene in the DMF/water solution led to the formation of elongated polystyrene species decorated with patchy nanospheres (inset to Fig. 4d).

We have thus developed a new strategy for nanoparticle surface patterning that is governed by thermodynamically controlled segregation of polymer ligands in pinned micelles with a footprint area comparable with the nanoparticle surface area. Polymer segregation is favoured for small nanoparticles with a large surface curvature. The experimental results were in excellent agreement with the proposed theoretical model. The described patterning strategy can be used for the generation of reconfigurable nanocolloids: reversible transitions between a smooth polymer shell and surface patches can be triggered by illumination, change in temperature, ionic strength or pH of the solution, that is, the stimuli changing the solvent quality. On demand, polymer patches can be ‘locked’ by permanent crosslinking, which would suppress nanoparticle assembly[31] and enable the utilization of solutions with a higher nanoparticle concentration, thereby increasing the yield of patchy nanoparticles.

The utilization of block copolymers will facilitate nanoparticle patterning with a variety of pinned micelle structures, including comicelles, which may tailor new functionalities to

patchy nanoparticles. ‘Grafting-from’ surface functionalization[32] and fractionation of nanoparticles with a particular number of patches will enhance control over the number of patches per nanoparticle. Patterning of multicomponent nanoparticles and the self-assembly of patterned nanoparticles into complex, hierarchical structures are other directions to explore. Furthermore, given the remarkable progress in the synthesis of nanoparticles with different shapes, the proposed strategy enables fundamental studies of polymer segregation on surfaces with large curvatures or surfaces with multiple curvatures.

Supplementary Material

Refer to Web version on PubMed Central for supplementary material.

Acknowledgments

We thank the Connaught Foundation and the National Science and Engineering Research Council of Canada (Discovery and Canada Research Chair programmes) for financial support of this work. E.B.Z. acknowledges partial support from the Russian Foundation for Basic Research (grant 14-03-00372a) and from the Government of Russian Federation (grant 074-U01). M.R. acknowledges financial support from the National Science Foundation (grants DMR-1309892, DMR-1436201 and DMR-1121107), the National Institutes of Health (grants P01-HL108808 and 1UH2HL123645), and the Cystic Fibrosis Foundation. Research was in part carried out at the Center for Functional Nanomaterials, Brookhaven National Laboratory supported by the US Department of Energy, Office of Basic Energy Sciences (under contract number DE-SC0012704). R.M.C. acknowledges the Natural Sciences and Engineering Research Council of Canada for a PGS-D scholarship. A.K. acknowledges an Ontario Trillium Scholarship. We thank M. Michaelis and S. Lin for initiating preliminary experiments and I. Gourevich for help with imaging experiments.

References

1. Bianchi E, Blaak R, Likos CN. Patchy colloids: state of the art and perspectives. Phys. Chem. Chem. Phys. 2011; 13:6397–6410. [PubMed: 21331432]
2. Preisler Z, Vissers T, Munað G, Smallenburg F, Sciortino F. Equilibrium phases of one-patch colloids with short-range attractions. Soft Matter. 2014; 10:5121–5128. [PubMed: 24910167]
3. Chen Q, Bae SC, Granick S. Directed self-assembly of a colloidal kagome lattice. Nature. 2011; 469:381–384. [PubMed: 21248847]
4. Glotzer SC, Solomon MJ. Anisotropy of building blocks and their assembly into complex structures. Nat. Mater. 2007; 6:557–562. [PubMed: 17667968]
5. Gröschel AH, et al. Guided hierarchical co-assembly of soft patchy nanoparticles. Nature. 2013; 503:247–251. [PubMed: 24185010]
6. Kern N, Frenkel D. Fluid–fluid coexistence in colloidal systems with short-ranged strongly directional attraction. J. Chem. Phys. 2003; 118:9882–9889.
7. Binks BP. Particles as surfactants: similarities and differences. Curr. Opin. Colloid Interface. Sci. 2002; 7:21–41.
8. Chen T, Chen G, Xing S, Wu T, Chen H. Scalable routes to Janus Au-SiO2 and ternary Ag-Au-SiO2 nanoparticles. Chem. Mater. 2010; 22:3826–3828.
9. Wang Y, et al. Colloids with valence and specific directional bonding. Nature. 2012; 491:51–55. [PubMed: 23128225]
10. Pawar AB, Kretzschmar I. Fabrication, assembly, and application of patchy particles. Macromol. Rapid Commun. 2010; 31:150–168. [PubMed: 21590887]
11. Sacanna S, Pine DJ. Shape-anisotropic colloids: building blocks for complex assemblies. Curr. Opin. Colloid Interf. Sci. 2011; 16:96–105.
12. Nie ZH, Petukhova A, Kumacheva E. Properties and emerging applications of self-assembled structures of inorganic nanoparticles. Nat. Nanotechnol. 2010; 5:15–25. [PubMed: 20032986]

13. Lattuada M, Hatton TA. Synthesis, properties and applications of Janus nanoparticles. Nano Today. 2011; 6:286–308.
14. Andala DM, Shin SHR, Lee HY, Bishop KJM. Templated synthesis of amphiphilic nanoparticles at the liquid-liquid interface. ACS Nano. 2012; 6:1044–1050. [PubMed: 22214288]
15. Vilain C, Goettmann F, Moores A, Le Floch P, Sanchez C. Study of metal nanoparticles stabilised by mixed ligand shell: a striking blue shift of the surface-plasmon band evidencing the formation of Janus nanoparticles. J. Mater. Chem. 2007; 17:3509–3514.
16. Jackson AM, Myerson JW, Stellacci F. Spontaneous assembly of subnanometre ordered domains in the ligand shell of monolayer-protected nanoparticles. Nat. Mater. 2004; 3:330–336. [PubMed: 15098025]
17. Bao C, et al. Effect of molecular weight on lateral microphase separation of mixed homopolymer brushes grafted on silica particles. Macromolecules. 2014; 47:6824–6835.
18. Williams DRM. Grafted polymers in bad solvents: octopus surface micelles. J. Phys. II. 1993; 3:1313–1318.
19. Zhulina EB, Birshtein TM, Priamitsyn VA, Klushin LI. Inhomogeneous structure of collapsed polymer brushes under deformation. Macromolecules. 1995; 28:8612–8620.
20. Koutsos V, van der Vegte EW, Pelletier E, Stamouli A, Hadziioannou G. Structure of chemically end-grafted polymer chains studied by scanning force microscopy in bad-solvent conditions. Macromolecules. 1997; 30:4719–4726.
21. Choi BC, Choi S, Leckband DE. Poly(*N*-isopropyl acrylamide) brush topography: dependence on grafting conditions and temperature. Langmuir. 2013; 29:5841–5850. [PubMed: 23600842]
22. Erathodiyil N, Ying JY. Functionalization of inorganic nanoparticles for bioimaging applications. Acc. Chem. Res. 2011; 44:925–935. [PubMed: 21648430]
23. Minelli C, Lowe SB, Stevens MM. Engineering nanocomposite materials for cancer therapy. Small. 2010; 6:2336–2357. [PubMed: 20878632]
24. Saha K, Agasti SS, Kim C, Li X, Rotello VM. Gold nanoparticles in chemical and biological sensing. Chem. Rev. 2012; 112:2739–2779. [PubMed: 22295941]
25. Wolf BA, Willms MM. Measured and calculated solubility of polymers in mixed-solvents-co-non-solvency. Makromol. Chem. 1978; 179:2265–2277.
26. Bürgi T. Properties of the gold–sulphur interface: from self-assembled monolayers to clusters. Nanoscale. 2015; 7:15553–15567. [PubMed: 26360607]
27. Rubinstein, M.; Colby, RH. Polymer Physics. Vol. 53. Oxford Univ. Press; 2003.
28. Zohar N, Chuntonov L, Haran G. The simplest plasmonic molecules: metal nanoparticle dimers and trimers. J. Photochem. Photobiol. C. 2014; 21:26–39.
29. Choueiri R, Klinkova A, Thérien-Aubin H, Rubinstein M, Kumacheva E. Structural transitions in nanoparticle assemblies governed by competing nanoscale forces. J. Am. Chem. Soc. 2013; 135:10262–10265. [PubMed: 23806016]
30. Klinkova A, et al. Structural and optical properties of self-assembled chains of plasmonic nanocubes. Nano Lett. 2014; 14:6314–6321. [PubMed: 25275879]
31. Lukach A, Liu K, Thérien-Aubin H, Kumacheva E. Controlling the degree of polymerization, bond lengths and bond angles of plasmonic polymers. J. Am. Chem. Soc. 2012; 134:18853–18859. [PubMed: 23078101]
32. Khabibullin A, Mastan E, Matyjaszewski K, Zhu S. Surface-initiated atom transfer radical polymerization. Adv. Polym. Sci. 2015; 270:29–76.

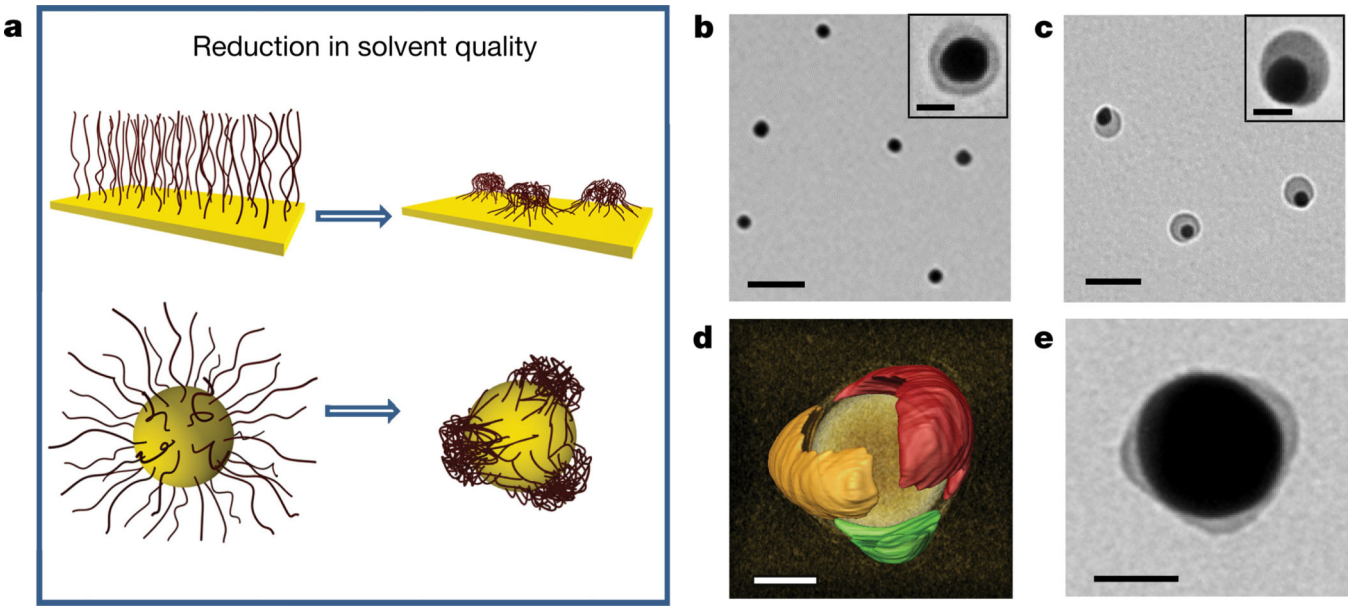

Figure 1. Polymer segregation on the nanoparticle surface

a, Schematics of solvent-mediated formation of pinned polymer micelles (surface patches) on a planar macroscopic surface (top) and on the nanoparticle surface (bottom). **b, c**, TEM images of gold nanospheres capped with polystyrene-50K at the grafting density of 0.03 chains per square nanometre and deposited on the grid from the 0.3 nM nanosphere solution in DMF (**b**) and from the DMF/water mixture at C_w = 4 vol% after 24 h incubation at 40 °C (**c**). Scale bars in **b** and **c** are 100 nm. Insets in **b** and **c** show the corresponding images of individual nanospheres. Inset scale bars are 20 nm. **d**, Electron tomography reconstruction image of the 60-nm-diameter nanosphere with three polystyrene-50K patches, each shown for clarity with a different arbitrary colour. The image of a gold core is removed to highlight the structure of polymer patches. The estimated resolution is 2–3 nm. Patchy nanospheres were formed as described in **c**. The grafting density of polystyrene-50K is 0.02 chains per square nanometre. **e**, TEM image of the gold nanosphere carrying photocrosslinked thiol-terminated polystyrene-*co*-polyisoprene patches preserved after 24 h incubation in tetrahydrofuran (a good solvent for polystyrene-*co*-polyisoprene). Original patchy nanoparticles were formed and crosslinked in the DMF/water mixture at C_w = 1 vol%. Scale bars in **d** and **e** are 20 nm.

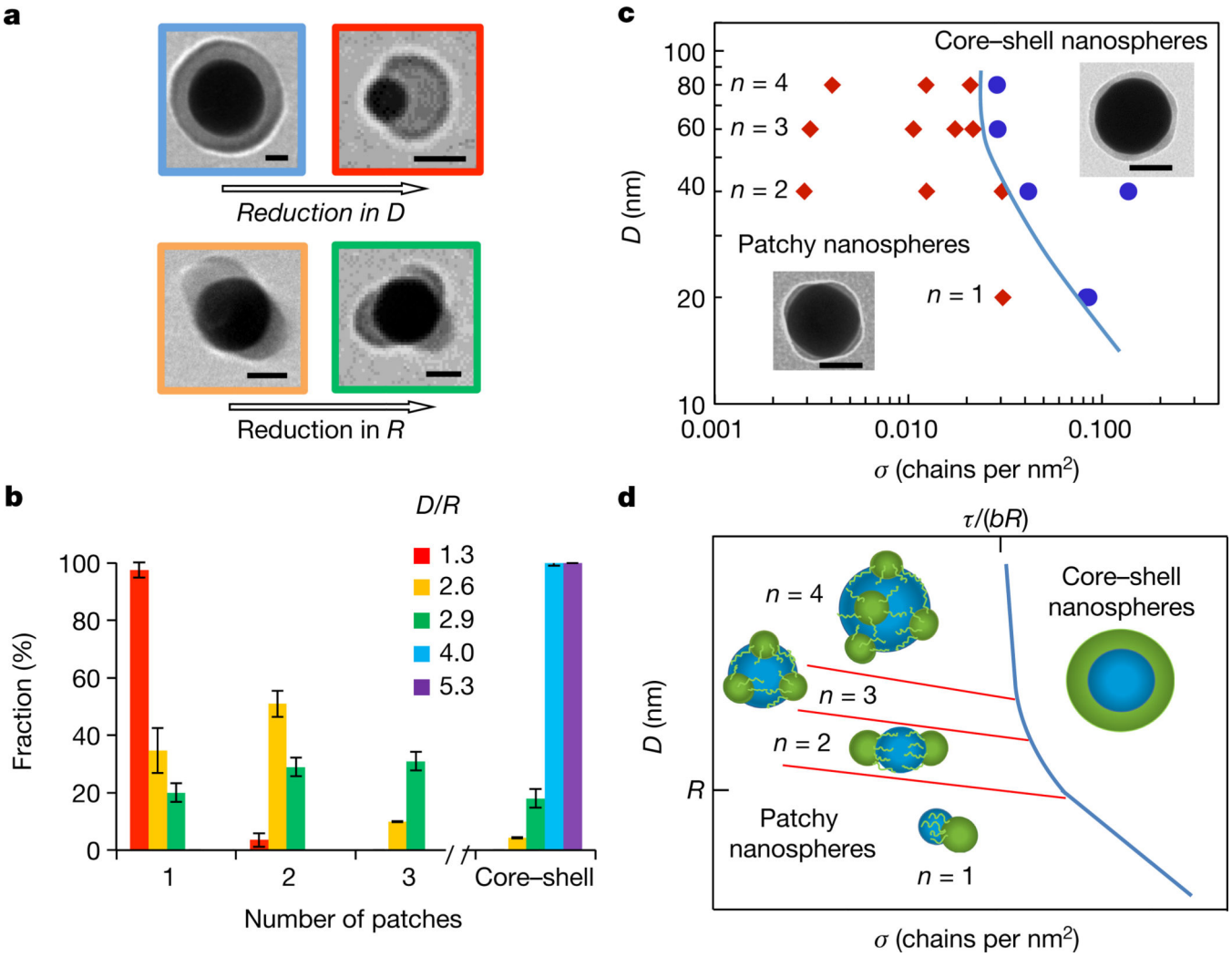

Figure 2. Structural transitions in the polymer layer on the surface of gold nanospheres

a, Effect of nanosphere size (top) and polymer dimensions (bottom) on patch formation. The nanospheres are functionalized with polystyrene-50K (top row and bottom left) and polystyrene-30K (bottom right) at σ = 0.03 chains per square nanometre. Scale bars are 25 nm. **b**, Distribution of populations of nanospheres with a different patch number. The red, yellow, blue and violet bars correspond to the 20-, 40-, 60- and 80-nm-diameter nanospheres capped with polystyrene-50K, respectively; the green bar represents 32-nmdiameter nanospheres functionalized with polystyrene-30K. σ = 0.03 chains per square nanometre. The error bars represent the standard deviations. Each experiment was run in triplicate. The inset shows the*D/R* ratios, with colours corresponding to the colours of bars and the frames of the images in **a**. **c**, Experimental diagram of nanosphere states. The blue line separates the regions of core–shell and patchy nanospheres with a different average patch number *n*. The insets illustrate patchy and a core– shell nanospheres with σ of 0.012 and 0.03 chains per square nanometre, respectively. Scale bars are 50 nm. In **b** and **c**, 200–300 nanospheres were analysed for each population. **d**, Theoretical diagram of nanosphere states. Transitions between nanospheres with different values of *n* begin at $D \approx R$ (red lines). The blue line

shows the boundary between the smooth and patchy polymer layer, approaching the grafting density $\sigma = \tau/(bR)$ for large nanospheres, similar to **c**.

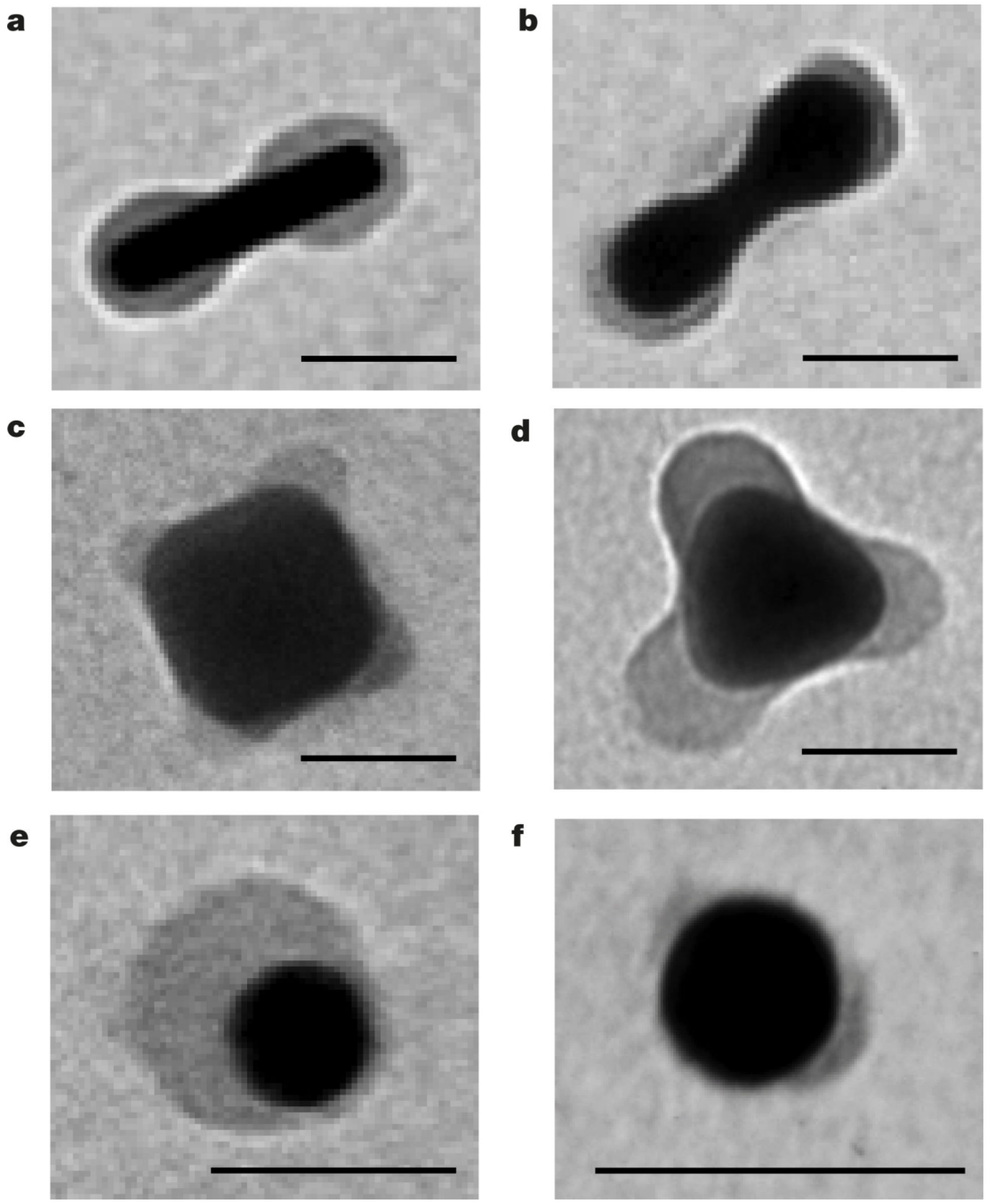

Figure 3. Generality of polymer patterning of nanoparticle surface

a–d, TEM images of polystyrene-50K-coated gold spherocylindrical nanorods (**a**), gold dumbbell-shaped nanorods (**b**), silver nanocubes (**c**) and silver triangular prisms (**d**), all in the DMF/water mixture at C_w = 4 vol%. **e, f**, TEM images of thiol-terminated poly(4-vinyl pyridine) (M_n = 22,000 g mol^{-1}) in water at pH = 10.5 (**e**) and thiol-terminated poly(*N*-vinylcarbazole) (M_n = 19,800 g mol^{-1}) in the DMF/water mixture at C_w = 4 vol% (**f**), both on the surface of gold nanospheres. All scale bars are 40 nm.

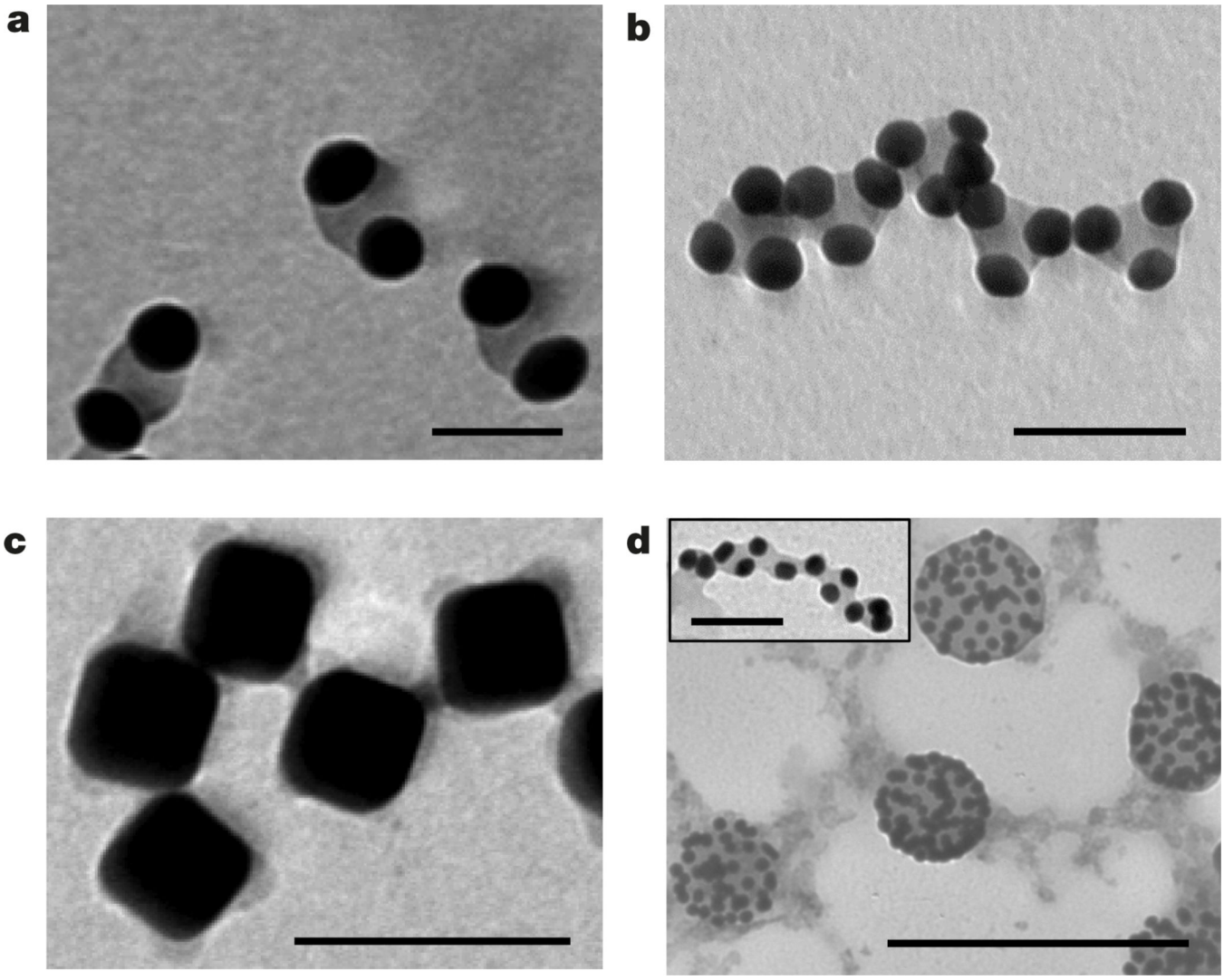

Figure 4. Self-assembly of patterned nanoparticles

a, Dimers of single-patch gold nanospheres. **b**, Self-assembly of trimers of single-patch gold nanospheres in chains. In **a** and **b** the nanospheres were capped with polystyrene-50K and incubated for 15 days in the DMF/water solution at C_w = 4 vol% at 40 °C. Scale bars in **a** and **b** are 40 nm. **c**, Self-assembly of patchy silver nanocubes functionalized with polystyrene-50K in the DMF/water mixture at C_w = 20 vol%; scale bar is 100 nm. **d**, Self-assembly of gold nanospheres on the surface of droplets enriched with free nonthiolated polystyrene. The self-assembly was induced by adding water at C_w = 4 vol% to the mixed solution of free non-thiolated polystyrene (M_n = 50,000 g mol^{-1}) and gold nanospheres tethered with polystyrene- 50K in DMF; scale bar is 250 nm. The inset to **d** shows self-assembly of patchy polystyrene-50K-capped gold nanospheres in the DMF/water mixture at C_w = 4 vol% in the presence of 0.625 nM of non-thiolated polystyrene, following 5 min sonication of the solution. Scale bar is 40 nm.